Sedimentology (2006) **53,** 597–609 doi: 10.1111/j.1365-3091.2006.00775.x

On the effect of moisture bonding forces in air-dry soils on threshold friction velocity of wind erosion

SUJITH RAVI*, TED M. ZOBECK†, THOMAS M. OVER‡, GREGORY S. OKIN* and PAOLO D'ODORICO*

**Department of Environmental Sciences, University of Virginia, 291 McCormick Road, Box 4000123, Charlottesville, VA 22904-4123, USA (E-mail: sujith@virginia.edu)*

†Wind Erosion and Water Conservation Research Unit, USDA, Agricultural Research Service, 3810 4th Street, Lubbock, TX 79415, USA

‡Department of Geology/Geography, Eastern Illinois University 600 Lincoln Ave, Charleston, IL 61920, USA

ABSTRACT

Wind erosion is a dominant geomorphological process in arid and semi-arid regions with major impacts on regional climate and desertification. The erosion process occurs when the wind speed exceeds a certain threshold value, which depends on a number of factors including surface soil moisture. The understanding and modelling of aeolian erosion requires a better understanding of the soil erodibility associated with different moisture conditions. In arid regions during the dry season, the atmospheric humidity plays an important role in determining the surface moisture content and the threshold shear velocity. By a series of wind tunnel tests and theoretical analyses, this dependence of threshold velocity on near surface air humidity is shown for three soils of different textures: sand, sandy loam, and clay loam. The results show that the threshold shear velocity decreases with increasing values of relative humidity for values of relative humidity between about 40% and 65%, while above and below this range the threshold shear velocity increases with air humidity. A theoretical framework is developed to explain these dependencies assuming an equilibrium between the surface soil moisture and the humidity of the overlying atmosphere. The conditions under which soil-atmosphere equilibrium occurs were tested experimentally in the laboratory for different soils in order to determine the effect of grain surface area and texture on the time required to reach equilibrium starting from different initial conditions.

Keywords Aeolian processes, desertification, soil moisture, wind erosion.

INTRODUCTION

Wind erosion is the wind-forced movement of soil particles and involves the entrainment, transport and deposition of soil grains by the air stream. This process, which depends on geological, climatic and land cover conditions, is known for being a major cause of land degradation in arid and semi-arid regions, in that it removes the fertile topsoil particles (Zobeck & Fryrear, 1986; Zobeck *et al.*, 1989) and damages vegetation. Moreover, dust emissions resulting from wind erosion are a major source of atmospheric aerosols, which affect both the air quality (Pope *et al.*, 1996) and the global radiation budgets (e.g. Ramanathan *et al.*, 2001) thereby contributing to changes in the regional and global climate. Grazing pressure, land degradation, and the lack of adequate soil conservation practices may render soils in arid and semi-arid regions more susceptible to wind erosion with important impacts on regional climate and desertification (e.g. Nicholson, 2000).

The physics of wind erosion is complex, as it involves atmospheric, soil and land surface processes (Shao, 2000). Even though the erosive action of the wind depends on its speed, several factors like field surface conditions, size and stability of the soil aggregates, clay content,

vegetation cover and near-surface soil moisture affect the threshold velocity, which is the minimum wind velocity required to cause erosion.

Aeolian erosion is particularly important in arid and semi-arid regions because the soils are generally dry and have sparse vegetation cover. Temporal variability of both vegetation cover and surface soil moisture is associated with changes in soil susceptibility to wind erosion. The understanding and modelling of aeolian erosion (for example, under climate change scenarios) requires a better understanding of the soil erodibility associated with different moisture conditions. In particular, during rainless periods, changes in surface soil moisture (here 'soil moisture' indicates the water content associated with the liquid phase only) are a result of fluctuations in air humidity. Wind tunnel tests have shown (Darwish, 1991; Ravi *et al.*, 2004) that atmospheric humidity plays an important role in determining the surface moisture content and the threshold shear velocity. In particular, Ravi *et al.* (2004) focused on air-dry soils and found that the threshold shear velocity is a decreasing function of the specific humidity measured in the air near the soil surface. This paper will further test the hypothesis that, when surface soil moisture is in equilibrium with the humidity (and temperature) of the overlying atmosphere, the threshold velocity in air-dry soils (i.e. those with soil matric potentials $\psi_m < -30$ to -100 MPa) decreases with the air humidity, while in more humid soils it increases. A theoretical framework is provided for the interpretation of these results based on the presence or absence of liquid bridges between soil particles, and of the bonding forces due to capillarity. This framework explains the nature of the dependence of threshold friction velocity on air humidity. The results are shown of a number of laboratory tests carried out to assess under what conditions the soil surface (a few-grain layers thick) can be considered to be in equilibrium with the atmosphere and to determine how long different soil types take to attain these equilibrium conditions, starting from different initial moisture contents.

WET BONDING EFFECTS ON THE THRESHOLD VELOCITY

Soil erosion occurs when the wind speed (u) exceeds a certain threshold value (u_t) that is sufficient to overcome the resistance of soil aggregates to detachment and removal. This threshold velocity depends on field surface conditions, surface roughness, size and shape of the soil aggregates and soil clay content, as well as near surface soil water content (e.g. Chepil, 1945; Belly, 1964). Studies on the threshold conditions for wind erosion usually use friction velocities (u^*) instead of wind velocities because they are directly related to the shear stress exherted on the surface. Both theoretical (Bagnold, 1941; Gregory & Darwish, 1989; McKenna Neuman & Nickling, 1989; Fecan *et al.*, 1999; Cornelis *et al.*, 2003) and empirical (Chepil, 1956; Belly, 1964; Bisal & Hsieh, 1966; Saleh & Fryrear, 1995) equations have been suggested in the past to express the threshold friction velocity (u_t^*) as a function of the water content at the soil surface.

The theoretical approach involves deriving an equation for threshold friction velocity (u_t^*) from the balance of forces acting on a soil particle at the threshold point, i.e. in critical conditions for the initiation of particle motion. A soil particle at the surface is subjected to several forces, including destabilizing forces exerted by the air stream – namely aerodynamic drag (F_d) and aerodynamic lift (F_l) – and stabilizing (or retarding) forces, such as gravity (F_g) and the interparticle cohesion force (F_i) (Shao, 2000). At the critical conditions for particle motion $u^* = u_t^*$, and there exists a balance between the retarding forces and aerodynamic forces, and the summation of moments about the pivot point is zero, i.e.

$$a_d F_d + a_g(F_l - F_g) - a_i F_i = 0, \qquad (1)$$

where a_d, a_g, a_i are dimensionless coefficients expressing the ratios between the force arms, r_d, r_g, r_i (of F_d, F_g and F_i), and the particle diameter (d). The early theoretical models referred to soil particles with spherical geometry: Bagnold (1941) derived an expression for the threshold velocity for dry soils, considering only the effect of aerodynamic drag and gravity, i.e.

$$a_d F_d - a_g F_g = 0. \qquad (2)$$

The drag force can be expressed as $F_d = \tau A_p$, with τ being the shear stress and A_p the projected area of the (spherical) particle. Thus the drag force can be expressed as $F_d = Cd^2\rho_a u^{*2}$, with u^* being the friction velocity of the air stream, ρ_a the air density, and C the drag coefficient. The gravity force is the (immersed) weight of the soil particle, $F_g = C_g d^3 g(\rho_s - \rho_a)$, with ρ_s being the density of the soil grains and C_g a shape factor. The Bagnold's threshold friction velocity (u_b^*) for dry soils can be obtained from Eq. 2:

$$u_{\mathrm{b}}^{*} = A\sqrt{\frac{\rho_{\mathrm{s}} - \rho_{\mathrm{a}}}{\rho_{\mathrm{a}}} gd}, \tag{3}$$

where A is given by

$$A = \sqrt{\frac{C_{\mathrm{g}} a_{\mathrm{d}}}{C a_{\mathrm{g}}}}. \tag{4}$$

Eq. 3 does not include the interparticle forces acting between soil grains, which are particularly important in the case of fine textured soils (Shao, 2000). When the interparticle forces (F_{i}) are included, Eq. 3 becomes

$$u_{\mathrm{t}}^{*} = u_{\mathrm{b}}^{*}\sqrt{1 + \frac{F_{\mathrm{i}} B}{(\rho_{\mathrm{s}} - \rho_{\mathrm{a}}) g d^{3}}} \tag{5}$$

with $B = a_{\mathrm{i}}/C_{\mathrm{g}} a_{\mathrm{g}}$.

The interparticle forces that bind soil particles together are electrostatic forces, van der Waal's forces, and forces due to presence of moisture in the area of contact between the adjacent grains (e.g. Cornelis, 2002). Haines (1925) and Fisher (1926) expressed wet-soil cohesion due to capillarity (liquid-bridge bonding) as a function of soil matric potential for spherical particles. McKenna Neuman & Nickling (1989) assumed the interparticle contact areas of the adjacent soil grains to be dissymmetric cones and developed a model to express the interparticle capillary forces. This geometrical approximation of the interparticle contact areas accounts only for liquid-bridge bonding between adjacent soil grains which is dominant in humid soils and not for the adsorbed-layer bonding of hygroscopic forces which is dominant in air-dry soils. Whether through liquid-bridge or adsorbed-layer bonding, moisture directly contributes to the interparticle forces and significantly affects the entrainment and supply of grains to the air stream (e.g. Belly, 1964). For sandy soils the interparticle forces contributed by this adsorbed layer are negligible when the soil is relatively wet, while adsorbed water may have a significant influence in relatively dry, clayey soils. Thus, McKenna Neuman & Nickling's (1989) model was applicable only to sandy soils. Fecan *et al.* (1999) generalized McKenna Neuman & Nickling's (1989) equation to the case of clayey soils; however, they did not explicitly account for interparticle adhesion forces. These forces were included by Cornelis *et al.* (2003), who accounted for van der Waal's and wet-bonding forces, including both adhesion and capillarity; capillarity was expressed without prescribing the geometry (neither conical nor spherical) of the interparticle contact areas.

In high soil moisture conditions the capillary forces dominate and liquid bridges exist between the soil grains. In air-dry soils which are characteristic of arid regions during the dry season, the adsorption forces dominate under low humidity conditions, as the moisture content is not sufficient for the formation of liquid bridges between soil grains. In these soils under low humidity conditions the capillary forces are negligible. At higher air humidity conditions a transition takes place with regard to which interparticle forces are dominant between adsorption and capillary forces. In these humidity conditions the water vapor starts condensing in the interparticle spaces between soil grains resulting in the formation of liquid bridges between soil grains (Fig. 1). The transition between conditions in which water is held within the soil only in the adsorbed layer to those in which liquid bridges are formed, is reported to occur for matric potentials of the order of about −30 (Harnby, 1992) to −100 MPa (Hilhorst *et al.*, 2001), which are characteristic of air-dry soils (e.g. Campbell & Norman, 1997). This corresponds to relative humidities of about 48% to 65% at equilibrium conditions.

For most of the existing models (Gregory & Darwish, 1989; Cornelis *et al.*, 2003; McKenna Neuman, 2003), wind tunnel experiments were carried out to determine the parameters needed to express threshold friction velocity as a function of soil moisture. These experiments were often performed using wetted soils, which were not in equilibrium with the atmospheric humidity and were thus affected by significant evaporation and

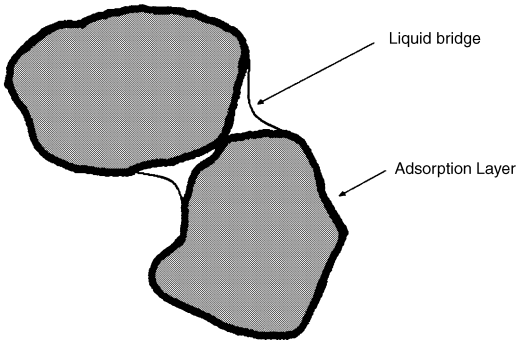

Fig. 1. Schematic illustrating soil water held in liquid bridges and in the adsorption layer. In air-dry soils (RH < 65%), the adsorptive component dominates the wet bonding forces because the soils are too dry for the liquid bridge bond to exist. In higher humidity conditions (RH > 65%) water condenses into liquid bridges between the soil grains and then the liquid bridge bonding dominates the wet bonding forces.

soil drying in the course of the tests. Gregory & Darwish (1989) and Dong *et al.* (2002) noticed that, because the threshold velocity is affected by the moisture content of the surface soil (a layer a few grains thick), the drying of the soil surface during wind tunnel tests may significantly affect the results. Gregory & Darwish (1989) also found that threshold velocities were affected by air humidity, suggesting that atmospheric variables such as temperature and specific humidity could be more easily used as predictors of soil erodibility than surface soil moisture, due to the difficulties commonly experienced in the accurate measurement of surface soil water content. This approach was recently followed by McKenna Neuman (2003), who investigated the effect of temperature and specific humidity on threshold friction velocity in relatively dry soils.

This paper presents an investigation of the effect of near-surface air humidity on the erodibility of both relatively dry soils, where wet-bonding forces are mostly contributed by hygroscopic water, and relatively wet soils, where interparticle forces are mostly due to capillarity. The dependence of wind erosion threshold on near-surface humidity was studied for both moisture regimes through a number of laboratory and wind tunnel experiments for three different soils. A theoretical framework is also developed in support of the results. Further, the conditions under which soil-atmosphere equilibrium occurs were tested experimentally in the laboratory, as the theoretical framework is developed assuming an equilibrium between the surface soil moisture and the overlying atmosphere. The equilibrium conditions are tested for different soils in order to determine the effect of grain surface area and texture on the time required to reach equilibrium starting from different initial conditions.

METHODS

General characterization of the soils

Three soils were studied: Brownfield sand, Pullman clay loam and Olton sandy loam. To study how the transition to equilibrium varies within the same textural class, three more sandy soils were considered in the laboratory analysis described below (Table 1). The soils were collected from different locations and air-dried at about 40 °C. The samples were crushed and sieved (2 mm sieve) a few days before the test. The moisture retention curves (Fig. 2) for the

Table 1. Classification and physical properties of the soils used in this study.

Soil series	Soil taxonomic class (USDA, 2004)	Soil texture	Grain size distribution (wet)			Specific surface area σ ($m^2\ g^{-1}$)
			% Sand (0·05–2·0 mm)	% Silt (0·002–0·05 mm)	% Clay (<0·002 mm)	
Pullman	Fine, mixed, superactive, thermic Torrertic Paleustolls	Clay loam	43	26	31	21·88
Olton	Fine, mixed, superactive, thermic Aridic Paleustolls	Sandy loam	70	13	17	15·39
Brownfield	Loamy, mixed, superactive, thermic Arenic Aridic Paleustalfs	Sand	92	0	8	6·97
Kalahari	Sand (not classified by USDA)	Sand	96	1	3	3·14
Plainfield	Mixed, mesic Typic Udipsamments	Sand	98	1	1	<1
Ottawa (US silica)	Uniform shaped and naturally rounded sand (quartz) particles	Sand	99	0	0	0·007

three soil types were determined by measuring the water potential values (using a water activity meter, DECAGON AquaLab Series 3T; DECAGON Devices, Pullman, WA, USA) and moisture content (gravimetrically). The water activity meter used in this study measures relative humidity through automated dew point instrumentation and can determine soil matric potentials above −300 MPa with an accuracy of ±0·003 water activity units (Gee *et al.*, 1992). Water activity readings, $a_w = \mathrm{RH}/100$ (with RH being the relative humidity), were converted into matric potential values as (Edlefson & Anderson, 1943):

$$\psi_m = \frac{RT}{M_w} \ln\left(\frac{\mathrm{RH}}{100}\right), \quad (6)$$

where R is the universal gas constant, T the absolute temperature and M_w is the molecular mass of water. The particle size distributions of the soils were determined using a Beckman-Coulter LS230 particle size analyser (Variable Speed Fluid Modular Plus; Beckman Coulter, Fullerton, CA, USA). Table 1 reports the results of the particle size analysis for the three soils. The specific surface areas of the soils were determined using a Gemini 2360 Surface Area Analyzer (Micromeritics Instrument Corp., Norcross, GA, USA) (Table 1). This instrument can accurately measure specific surface areas in the range 0·1–300 $m^2\ g^{-1}$ with an accuracy of ±0·5%. The samples were made free of moisture and other contaminants before the surface area analysis using a degasser (Flow Prep 060; Micromeritics Instrument Corp.).

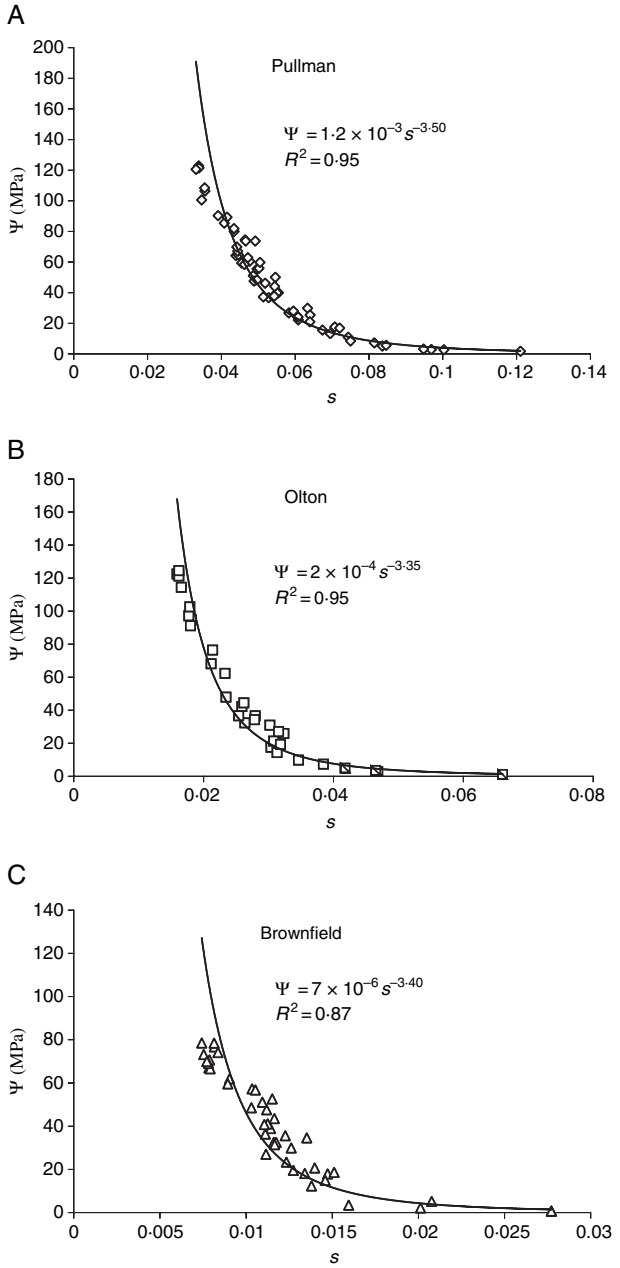

Fig. 2. Water retention curves for the three main soil types used in this study: (A) Pullman, (B) Olton and (C) Brownfield.

Analysis of the transition to equilibrium laboratory ambient conditions (RH ≈ 60% and $T \approx 21$ °C)

Gravimetric study of the transition from wet or oven-dry conditions to equilibrium with ambient conditions

A procedure, which is described below, was used to estimate the time needed to reach equilibrium of soil moisture content with ambient RH and temperature conditions beginning from wetted and oven-dried states, and to compare these values between different soils within the same texture class. To this end, six soils – Pullman, Olton, Brownfield, Kalahari, Ottawa and Plainfield – were tested. Samples (2 mm thick) of each soil were taken in 4 cm diameter metal cups, and the initial sample weight was recorded. The samples were wetted using a sprayer and allowed to absorb the moisture for 5–10 min. Each sample was then placed on a weighing balance, and the weight was noted at periodic intervals until it was approximately equal to the initial, unwetted soil. The same soil cup was then dried in an oven at 105 °C for 12 h. The oven-dry soil was cooled for 1 min at ambient conditions (60% RH and 21 °C) and placed on the weighing balance, and the weight was noted at periodical intervals until the weight became approximately equal to that of the initial air-dry, unwetted value.

Gravimetric study of the transition from wet conditions to equilibrium with ambient conditions on thick soil samples

To understand more clearly whether and how the thickness of the soil column affects the transition from wetted to ambient conditions a similar experiment was carried out on soil samples thicker than 2 mm. In this case, each soil was spread 2 cm deep on two metal trays ($48 \times 28 \times 2$ cm) and allowed to equilibrate with the ambient atmospheric conditions for 8–12 h. The top 2 mm of the soil from both trays was sampled, and the moisture content was measured gravimetrically. One of the trays was then wetted using a fine sprayer and the soil was allowed to absorb moisture for 5 min. The other tray was allowed to remain unwetted as a control. The top 2 mm of the soil from both trays was sampled periodically, and the moisture content of the sample was measured gravimetrically. This process was continued until the surface soil moisture was found to be approximately equal to the surface soil moisture in the control tray, thus matching ambient conditions. This experiment gives an estimate of how long each soil takes to reach the equilibrium with ambient conditions after a wetting event.

Study of the transition from oven-dry to equilibrium through water potential measurements

To check whether the equilibrium conditions are independent of the initial surface soil moisture, changes in water potential were measured from oven-dry to ambient conditions for three soil samples of each soil type. Three samples (2 mm thick) of each soil were placed in 4 cm diameter metal cups and oven dried at 105 °C for 12 h, while three control cups of each soil were kept in ambient conditions. The cups were taken out of the oven and allowed to cool at ambient conditions for 5–10 min. The water activity of each soil sample was measured using the water activity meter at constant intervals of 5 min until the water activity readings were found to be approximately equal to the water activity values of the control samples kept in ambient conditions.

Wind tunnel tests

This study used a non-recirculating wind tunnel, 10·0 m long by 0·5 m wide by 1·0 m high, housed at the Cropping Systems Research Laboratory of the USDA (Agricultural Research Service in Lubbock, TX, USA). The test section has plexiglass windows and was equipped with removable metal trays ($1{\cdot}5 \times 46 \times 100$ cm). The bottom of the tunnel was covered with a sand paper lining with approximately the same roughness as the soil surface in the tray. The air stream was generated by a fan at the end of the tunnel powered by an electric motor (see, e.g. Orozco, 2000 for a complete description of this wind tunnel). A series of Pitot tubes mounted on a rack at different heights inside the tunnel immediately in front (upwind) of the test section and connected to different ports of a SCANIVALVE[1] pressure transducer array (SCANIVALVE Corp., Liberty Lake, WA, USA) were used to estimate the wind velocity as a function of height inside the wind tunnel. These velocity values were used to calculate the parameters of the wind profile and to express the wind speed in terms of friction velocity. To this end, least square regression was used to fit the Prandtl logarithmic law to the measured wind speed profile. During the soil erosion tests the Pitot tube array was removed and replaced with a single Pitot tube at a height of 60 cm. Initiation of saltation was measured using a SENSIT[1] impact sensor (e.g. Stout & Zobeck, 1997; http://www.lbk.ars.usda.gov/wewc/pdf/sensit.pdf; SENSIT Company, Portland, ND, USA) mounted on the floor of the wind tunnel 45 cm downwind from the test section, protruding 2·0 cm above the wind tunnel floor. Temperature and relative humidity were recorded by a probe (Humitter 50 U, accuracy of ±2% RH; Vaisala Inc., Woburn, MA, USA) placed 2 mm above the surface of the soil in the tray. Soil temperature was measured remotely using an infrared thermometer (IRT/C.2 with Type K Germanium lens; Exergen Corp. Watertown, MA, USA) mounted 90 cm above the soil surface. A wire thermocouple and a handheld relative humidity/temperature probe (Testo Model 610; Testo Inc., Flanders, NJ, USA) were used to determine ambient room temperature and relative humidity.

The soils were kept on trays (three replicates for each test on each soil type) and allowed to equilibrate with the atmosphere in the room with the wind tunnel for 8–12 h before each wind-tunnel test. The gravimetric soil moisture of the top 2 mm was measured after each test, while simultaneous measurements of gravimetric soil moisture were also made in a control tray for each soil type. These soils were neither artificially wetted nor dried, and

[1]Identification of experimental apparatus is for information purposes only and does not imply endorsement by ARS, USDA.

the only variations in surface moisture content were due to changes in the ambient air humidity and temperature. The climatic parameters were not controlled for these wind tunnel experiments. The experiments were run in ambient conditions on dry, cloudy and rainy days, in order to cover a fairly broad range of relative humidity. The air in Lubbock is generally dry and the stronger variability in air humidity is due to the diurnal cycle more than to seasonal fluctuations. The moisture content of the surface soil sampled from the control trays and the trays used for the wind tunnel tests showed good agreement suggesting that the experiments were not affected by significant soil drying during the tests.

Before each wind tunnel test the Pitot tube and its transducer were calibrated and corrections were made for changes in ambient temperature. The calibrations were made using a portable manometer connected in parallel to the Pitot tubes and the pressure transducer. The procedure for each test was as follows: a tray was placed in the wind tunnel, the test-section window was closed, the wind speed was initially increased rapidly to a wind speed just below the threshold value, and then the speed was increased slowly until the saltation sensor indicated particle movement. The threshold velocity was determined as the velocity at which an abrupt increase from zero to more than 100 particle impacts per second was observed. Observations from all the automated sensors were taken at 1 Hz frequency during triplicate tests of each soil. These data were corrected to account for the changes in ambient air pressure and their effect on wind velocity measurements with the Pitot tubes. To this end, air pressure values measured at a nearby (<1 km away) meteorological station were used.

RESULTS AND DISCUSSION

This paper studies the effect of atmospheric humidity on threshold friction velocity under the assumption that soils are in equilibrium with the overlying atmosphere. An equilibrium theory is also developed, which relates soil erodibility to relative humidity. It is thus fundamental to first assess under what conditions such equilibrium actually exists at the soil surface.

Transition to equilibrium conditions

The results of the gravimetric tests of the transition to equilibrium described above (Figs 3–5) indicate that the soil surface tends to equilibrium soil matric potential. Eq. 6 combined with the water retention curves (Fig. 2) provides the gravimetric soil moisture at equilibrium between the surface soil layer and the overlying air. Figure 3A–F shows the transition from wet and oven dry conditions to equilibrium with the ambient conditions for six different soil types (in the decreasing order of specific surface areas). These results (Table 2) indicate that the same equilibrium conditions are attained independently of the initial moisture content. The duration of the transition to equilibrium depends on the soil texture and the initial moisture content, with the longer transients being associated with the higher clay contents and thereby higher specific surface areas (Table 1). The results of the wetting experiments on thicker samples (Fig. 4) show this effect of soil texture in determining the time needed to reach equilibrium conditions. The Brownfield sand has the lowest clay content (and the smallest specific surface area: see Table 1) and hence the soil surface requires the shortest time to attain equilibrium. On the other extreme, the Pullman clay has the highest clay content (and the largest specific surface area) and takes the longest time to reach equilibrium (Table 3). The results of measurements with the water activity meter (Fig. 5) confirm the conclusion that equilibrium conditions are independent of the initial surface soil moisture. In fact, the three replicates for each soil type had different initial soil moisture contents but reached the same equilibrium conditions. The results shown in Figs 3–5 indicate that the time needed to reach equilibrium strongly depends on (increases with) clay content and with the specific surface area.

Wind-tunnel tests

Following the procedure described above, wind-tunnel tests were carried out to assess the dependence of threshold friction velocity on atmospheric humidity for three of the soils considered in this study. The soil moisture did not significantly change in the test trays during the wind-tunnel tests as compared to control trays sitting in the same room. This is shown in Fig. 6, in which values of (gravimetric) soil moisture (s_2) of samples taken from the test trays (top 2 mm) after the wind tunnel tests are plotted against soil moisture values of surface samples from the control trays (s_1), combining all tests on all soils (Fig. 6).

According to previous results (Ravi *et al.*, 2004), surface soil moisture, and hence the threshold shear velocity were more strongly

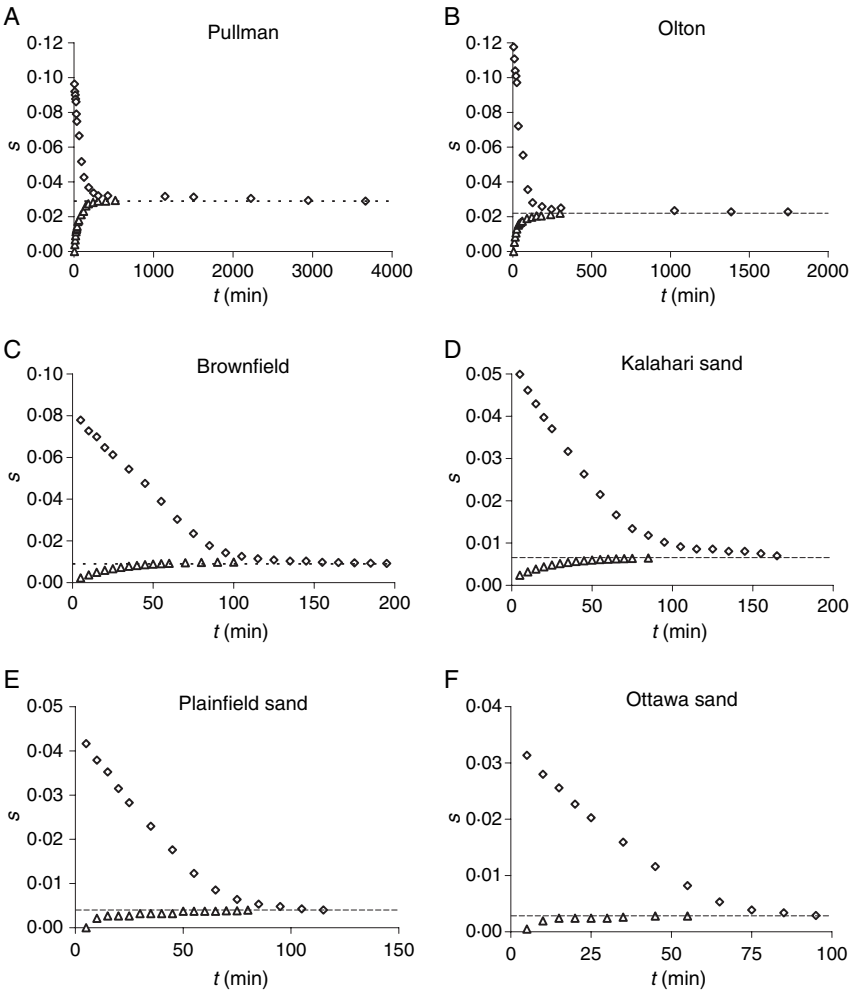

Fig. 3. Plots showing results of the gravimetric study of the transient from wet (diamonds) or oven-dry (triangles) conditions to equilibrium with ambient air humidity for six different soils: (A) Pullman clay loam, (B) Olton sandy loam, (C) Brownfield sand, (D) Kalahari sand, (E) Plainfield sand and (F) Ottawa sand. The dotted lines indicate the equilibrium conditions (see Table 2).

controlled by near-surface atmospheric humidity than by soil temperature. In fact, the only dependence detected on surface temperature was a consequence of the negative correlation between temperature and air humidity in the set of environmental conditions in which the tests were performed.

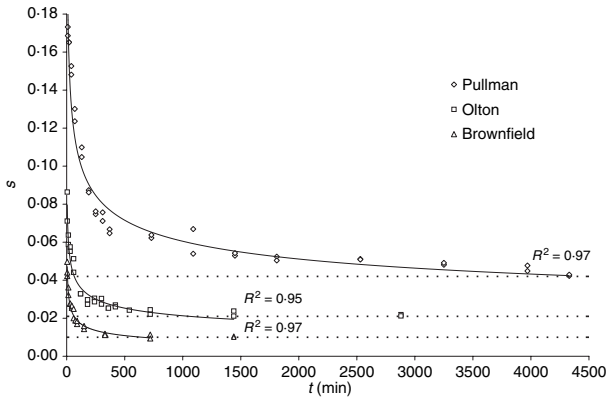

Fig. 4. Plot showing results of a gravimetric study of the transition from wet conditions to equilibrium with ambient conditions sampling the top 2 mm from 2 cm deep soil trays. The dotted lines indicate the equilibrium conditions, the solid lines represent an exponential fit.

The primary experimental result found in this study is that for the three soils studied, threshold friction velocity increases with an increase in air humidity at very low and high humidity, while in the middle humidity range the threshold velocity decreases with increasing air humidity. These results are shown in Fig. 7, where threshold wind speed values are averaged within classes of relative humidity covering a range between 10% and 90%. This pattern appears to be particularly well defined in the case of soils richer in clay content. The existence of a region where the threshold velocity decreases with humidity seems to be counterintuitive, as the threshold velocity is commonly expected to increase with the surface soil moisture (e.g. Cornelis & Gabriels, 2003) and, hence also with the atmospheric humidity. However,

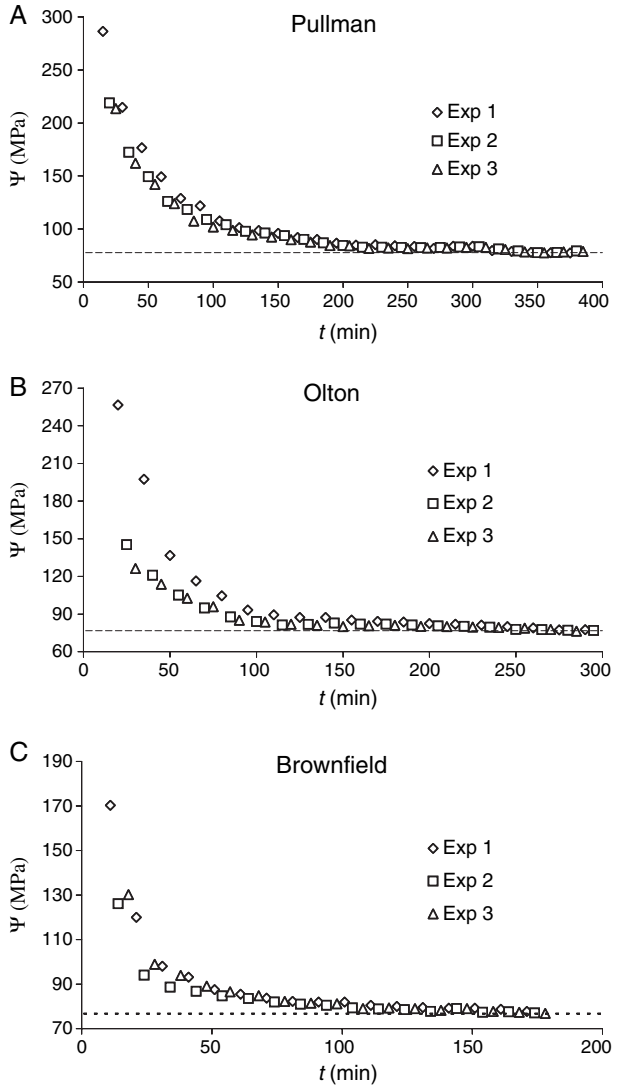

Fig. 5. Transition from oven-dry to equilibrium expressed through water potential measurements for three different soil types: (A) Pullman clay loam, (B) Olton sandy loam and (C) Brownfield sand. The dotted lines indicate the equilibrium conditions.

these results can be explained on the basis of the theory of wet bonding forces and their effect on threshold velocity.

McKenna Neuman (2003) modified the Shao–Lu threshold model (Shao & Lu, 2000) to derive an expression for interparticle bonding forces as:

$$F_i = \beta_c d + |\psi_m| A_c, \qquad (7)$$

where β_c is a dimensional parameter with units N m^{-1}, d is the particle diameter, ψ_m is the matric potential and A_c is the wet contact area between adjacent grains. The term $\beta_c d$ accounts for van der Waal's and electrostatic forces, while $|\psi_m| A_c$ accounts for wet-bonding forces associated with the moisture content. In air-dry soils where adsorption forces dominate, the effect of capillarity is negligible and thus the effect of surface tension due to the curvature of the air-water interface is dropped from the equation. In this case, the water retained in the soil is held by surface adsorption of moisture as a film over the soil grains. In air dry soils the adsorptive forces dominate the wet bonding forces because the soils are too dry for liquid bridge bonding. In these conditions a small decrease in soil moisture is associated with a strong increase in absolute value of soil matric potential, with only a smaller change in the contact area (A_c) as shown in the following paragraphs. At higher air humidity, capillarity contributes to wet bonding because water condenses to form liquid bridges between soil grains. In this case, the effect of surface tension (Fisher, 1926) needs to be added to Eq. 7 because liquid-bridge bonding dominates the interparticle force. As a result, threshold friction velocity increases with an increase in relative humidity as previously noted by McKenna Neuman & Nickling (1989) and Cornelis *et al.* (2003), who showed that the liquid-bridge bonding force is inversely proportional to the absolute value of soil matric potential and, thus it increases with the soil water content.

For dry powders where wet bonding is only due to forces of adsorption between the water films coating the particles (Fig. 8), Harnby (1992) expressed the contact area of the adsorbed layers between two spherical grains as:

Table 2. Ambient moisture content and time required for transition to equilibrium conditions for the six different soil types using 2 mm thick soil samples as in Fig. 3. An initial moisture content (gravimetric) of 0·04 was used in the study of the wet-to-equilibrium transitions. The equilibrium soil moisture is the gravimetric soil moisture of the control samples.

Soil type	Gravimetric moisture at equilibrium	Time to equilibrium (from Fig. 3, in minutes)	
		Wet to equilibrium	Oven dry to equilibrium
Pullman	0·066	3540	520
Olton	0·022	1560	300
Brownfield	0·009	165	100
Kalahari	0·006	145	90
Plainfield	0·004	115	80
Ottawa	0·002	95	45

Table 3. Transition from 'wet' conditions to equilibrium (column 2) with ambient conditions (RH = 60% and $T = 21$ °C) for three soil types (gravimetric moisture of top 2 mm surface soil from 2 cm deep soil in trays). The theoretical (column 5) and experimental (column 4) water potential at equilibrium and the time (column 3) required to reach the equilibrium conditions (using a water activity meter) are also shown for the same soil types.

	Time to equilibrium (min)		Ψ at equilibrium (MPa)	
Soil type	Wet to equilibrium (thick soil sample as in Fig. 4)	Oven dry to equilibrium (using water potential measurements)	Experimental (Fig. 5)	Theoretical (Eq. 6)
Pullman	4000	520	−77·69	−74·26
Olton	1500	300	−75·96	−70·115
Brownfield	700	100	−74·95	−69·31

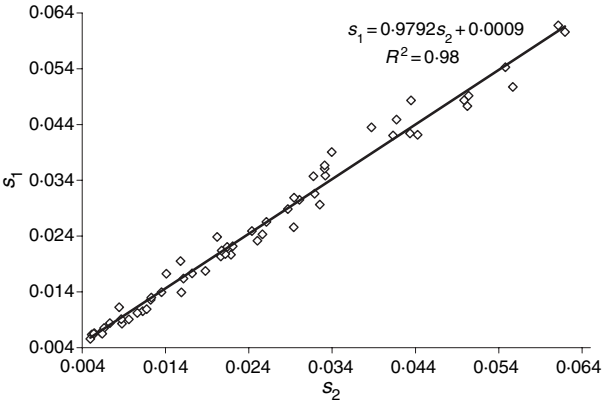

Fig. 6. Plot showing surface gravimetric soil moisture (top 2 mm) of control trays (s_1) and wind blown trays (s_2), determined gravimetrically.

$$A_c = 4\pi\left(\delta - \frac{y}{2}\right) R_2 \left(\frac{m}{m+1}\right), \quad (8)$$

where y is the distance between the surface of two spheres of radius R_1 and R_2, m is the ratio R_1/R_2, and δ is the average thickness of the adsorption film (Fig. 8). Assuming that the soil grains in contact are uniform spheres with $R_1 = R_2 = R$, Eq. 8 can be modified as:

$$A_c = 2\pi\left(\delta - \frac{y}{2}\right) R. \quad (9)$$

Thus the contact area is either zero if the thickness of the water film is less than half of the interparticle distance (i.e. $\delta < y/2$) otherwise it is given by Eq. 9. In this case, the interparticle forces in air-dry soils in the absence of liquid bridge forces (Eq. 7) can be expressed as:

$$F_i = \beta_c d + |\psi_m|_c \pi\left(\delta - \frac{y}{2}\right) d \quad \text{with} \quad \delta > \frac{y}{2}. \quad (10)$$

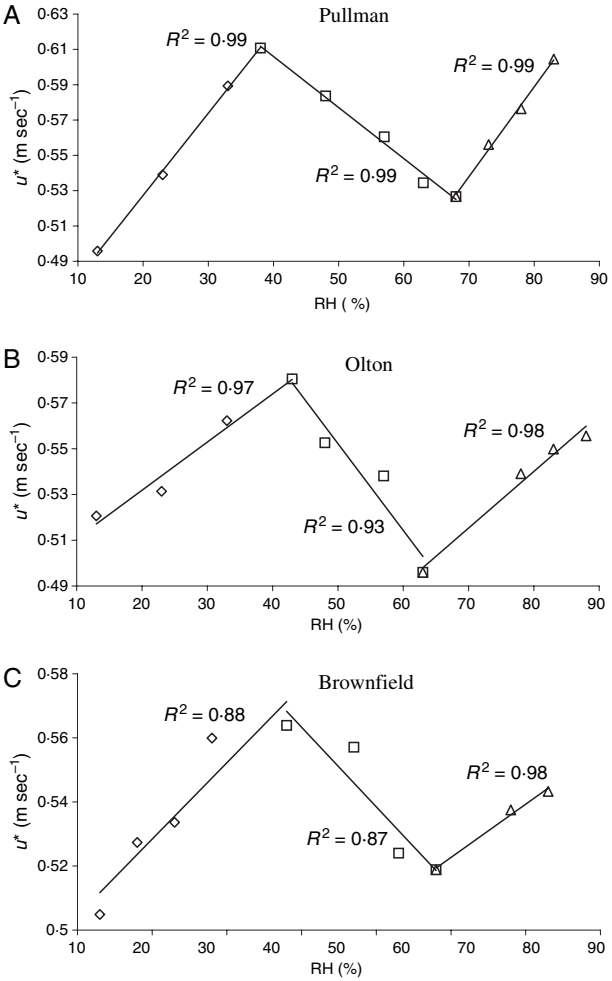

Fig. 7. Threshold shear velocity (u^*) as a function of relative humidity (RH) as determined by wind-tunnel tests for three soils (A) Pullman clay loam, (B) Olton sandy loam and (C) Brownfield sand. Values of u^* were averaged within classes of RH.

The average thickness of the adsorption film (δ) can be expressed in terms of gravimetric soil moisture, s (mass of water per mass of dry soil)

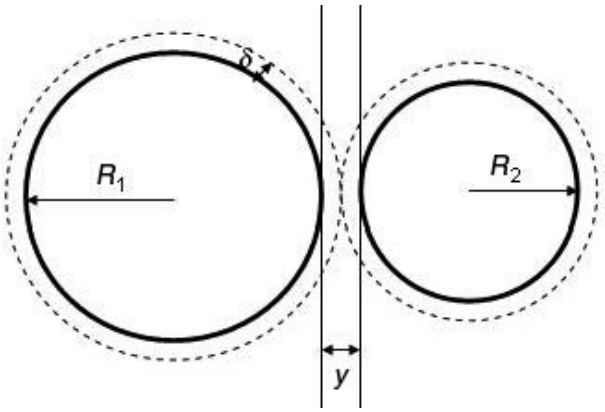

Fig. 8. Schematic showing two adjacent spherical soil grains with diameters R_1 and R_2 having an adsorption layer with thickness δ (which is a function of soil moisture); y is the spacing between the particles and is a function of soil packing (modified after Harnby, 1992).

and specific surface area, σ (total grain surface per unit mass), as:

$$\delta = \frac{s}{\rho_w \sigma}, \tag{11}$$

where ρ_w is the water density.

Eq. 10 can be rewritten as:

$$F_i = \beta_c d + \pi\left(\frac{s}{\rho_w\sigma} - \frac{y}{2}\right)|\psi_m| d \quad \text{if} \quad s > \frac{y}{2}\rho_w\sigma \tag{12}$$

and

$$F_i = \beta_c d \quad \text{if} \quad s < \frac{y}{2}\rho_w\sigma. \tag{13}$$

The loss of wet bonding component of F_i for low moisture contents [i.e. for $s < (y/2)\rho_w\sigma$] explains the decrease in threshold velocity with decreasing values of relative humidity observable in (Fig. 6) for RH < 40% shown in (Fig. 7) for lower values of RH. Equation 12 is now used to explain the dependence of threshold velocity on RH in the middle humidity range in Fig. 7. Using the Clapp & Hornberger (1978) parameterization, soil moisture (s) can be expressed as a function of matric potential as:

$$s = c|\psi|^{-b}. \tag{14}$$

Combining Eq. 14 with Eq. 6 – assuming the existence of equilibrium at the soil-air interface – an expression for adsorbed-layer bonding as a function of relative humidity is obtained,

$$F_i = d\left[\pi\left(\frac{c}{\rho_w\sigma}\left(\frac{RT}{M}\right)^{-b}\left(\ln\frac{RH}{100}\right)^{-b} - \frac{y}{2}\right)\right]\frac{RT}{M} \times \ln\left(\frac{RH}{100}\right) + \beta_c d. \tag{15}$$

Eq. 15 can be expressed also as:

$$F_i = dD\ln\left(\frac{RH}{100}\right) + \beta_c d, \tag{16}$$

where

$$D(RH) = \left[\pi\left(\frac{c}{\rho_w\sigma}\left(\frac{RT}{M}\right)^{-b}\left(\ln\frac{RH}{100}\right)^{-b} - \frac{y}{2}\right)\right]\frac{RT}{M}. \tag{17}$$

Notice D(RH) depends on relative humidity, soil texture, through the parameters a and b of the moisture retention curve, on the specific surface area (σ), and on the particle packing through the parameter y.

Substituting Eq. 16 in Eq. 5 gives:

$$u_t^* = u_b^*\sqrt{1 + \frac{B\left[D\ln\left(\frac{RH}{100}\right) + \beta_c\right]}{(\rho_s - \rho_a)gd^2}}. \tag{18}$$

Eqs 8–18 are based on the assumption of uniform and spherical soil particles and should be tested either on glass beads or soils with uniform grain size. The main shortcoming of the above framework in soils with a broad range of particle sizes is that it does not account for the fact that in air-dry conditions most of the available soil moisture is retained by adsorption on the smaller clay particles. Moreover the only known relation between matric potential and relative humidity (Eq. 6) assumes the existence of equilibrium conditions between the soil surface and the near-surface atmosphere. Nevertheless, this approach (i.e. Eqs 8–18) provides at least a first conceptual framework in which to understand the dependence of threshold friction velocity on air humidity in the absence of liquid bridges. Eq. 18 shows that in air-dry soils u^* should decrease with increasing values of relative humidity, which explains the negative trend in (Fig. 7) for values of relative humidity between about 40% and 65%.

As noted before, for relative humidity >65% water condenses into liquid bridges and the effect of surface tension (Fisher, 1926) modifies the nature of the dependence of interparticle bonding on water content (McKenna Neuman & Nickling, 1989; Cornelis *et al.*, 2003). In this case u^* is expected to increase with air humidity, as demonstrated by McKenna Neuman (2003).

CONCLUSION

Using a sand, a sandy loam, and a clay loam soil, a series of wind-tunnel experiments was performed investigating the effect of air humidity on the threshold velocity of wind erosion for soils whose surface soil moistures were in equilibrium with the air. These experiments show that the threshold friction velocity decreases with increasing values of relative humidity for values of relative humidity between about 40% and 65%, while above and below this range the threshold friction velocity increases with air humidity. A theoretical framework was developed to explain these results. Another series of experiments was performed to test whether the soil surfaces were in equilibrium with the overlying atmosphere and also to determine the time needed to reach equilibrium, starting from both wet and dry initial conditions. Sands reached equilibrium within about 1–2 h starting from both wet and dry regimes, whereas clays were found to take several days to reach equilibrium starting from wet surface conditions. The analysis of the transition to equilibrium within the same texture class (sands) showed that the specific surface area is an important factor affecting the duration of these transients, i.e. the sandy soils with the larger particle surface area take a longer time to reach equilibrium with ambient conditions.

ACKNOWLEDGEMENTS

This research was supported by USDA (Cooperative Agreement No 2002-35102-11585) and NSF (EAR 0409305). Technical assistance was provided by Mr Dean Holder (Wind Erosion and Water Conservation Unit, Cropping Systems Research Laboratory, USDA-ARS, Lubbock, TX, USA). The authors gratefully acknowledge the contributions of Prof. James A. Smith and Dr Vinka Craver (Department of Civil Engineering, University of Virginia) who provided access to laboratory facilities and technical guidance.

NOMENCLATURE

A_c	wet contact area between adjacent grains (m^{-2})
a_d,a_g,a_i,a_l	ratio of moment arms lengths to the soil grain diameter (dimensionless)
a_w	water activity (dimensionless)
C	drag coefficient (dimensionless)
C_g	shape factor (dimensionless)
d	particle diameter (m)
F_d	drag force (N)
F_g	gravitational force (N)
F_l	lift force (N)
F_i	interparticle force (N)
g	acceleration due to gravity (m s^{-2})
M_w	molecular mass of water (kg)
R	universal gas constant (J mol^{-1} K^{-1})
R_1, R_2	radii of adjacent spherical soil grains (m)
RH	relative humidity (dimensionless, %)
T	temperature (Kelvin)
y	distance between the surface of two spheres of radius R_1 and R_2 (m)
u^*	threshold friction velocity (m s^{-1})
u_b^*	Bagnold's threshold velocity (m s^{-1})
β_c	dimensional parameter of electrostatic and van der Waal's forces (N m^{-1})
δ	average thickness of the adsorption film (m)
ψ_m	soil matric potential (MPa)
ρ_w	water density (kg m^{-3})
ρ_s	density of soil grain (kg m^{-3})
ρ_a	density of air (kg m^{-3})
σ	total grain surface per unit mass (m^2 g^{-1})
τ	shear stress of the air stream (N m^{-1})

REFERENCES

Bagnold, R.A. (1941) *The Physics of Blown Sand and Desert Dunes*. Methuen, London, 265 pp.

Belly, P.Y. (1964) *Sand Movement by Wind*, Technical Memorandum No. 1. U.S. Army Coastal Eng. Res. Center, Washington, D.C.

Bisal, F. and **J. Hsieh** (1966) Influence of soil moisture on erodibility of soil by wind. *Soil Sci.*, **102,** 143–146.

Campbell, G.S. and **J.M. Norman** (1997) *An Introduction to Environmental Biophysics*, 2nd edn. Springer, New York, 286 pp.

Chepil, W.S. (1945) Dynamics of wind erosion. I. Nature of movement of soil by wind. *Soil Sci.*, **60,** 305–320.

Chepil, W.S. (1956) Influence of soil moisture on erodibility of soil by wind. *Proc. Soil. Sci. Soc. Am.*, **20,** 288–292.

Clapp, R.B. and **Hornberger, G.M.** (1978) Empirical equations for some hydraulic properties. *Water Resour. Res.*, **14,** 601–604.

Cornelis, W.M. (2002), *Erosion process of dry and wet sediment induced by wind and wind driven rain: a wind-tunnel study*. PhD Dissertation, Ghent University, Ghent, Belgium.

Cornelis, W.M. and **Gabriels, D.** (2003) The effect of surface moisture on the entrainment of dune sand by wind: an evaluation of selected models. *Sedimentology*, **50,** 771–790.

Cornelis, W.M., Gabriels, D. and **Hartmann, R.** (2003) Parameterisation for the threshold shear velocity to initiate deflation of dry and wet sediment. *Geomorphology*, **59,** 43–51.

Darwish, M.M. (1991) *Threshold friction velocity: moisture and particle size effects*. MS Thesis, Texas Tech University, Lubbock, TX.

Dong, Z., Liu, X. and **Wang, X.** (2002) Wind initiation thresholds of the moistened sands. *Geophys. Res. Lett.*, **29,** No. 12, 1585, 10.1029/2001GL013128.

Edlefson, N.E. and **Anderson, A.B.C** (1943) Thermodynamics of soil moisture. *Hilgardia*, **15,** 31–298.

Fecan, F., Marticorena, B. and **Bergametti, G.** (1999) Parametrization of the increase of the aeolian erosion threshold wind friction velocity due to soil moisture for arid and semi-arid areas. *Ann. Geophys.*, **17,** 149–157.

Fisher, R.A. (1926) On the capillary forces in an ideal soil. Correction to formulae given by W. B. Haines. *J. Agric. Sci.*, **16,** 492–505.

Gee, G.W., Campbell, M.D., Campbell, G.S. and **Campbell, J.H.** (1992) Rapid measurement of low soil water potentials using a water activity meter. *Soil Sci. Soc. Am. J.*, **56,** 1068–1070.

Gregory, J.M. and **Darwish, M.M.** (1989) Threshold friction velocity prediction considering water content. *Proc. Am. Soc. Agric. Eng.*, Paper No. 90-2562. American Society of Agricultural Engineering, New Orleans, LA.

Haines, W.B. (1925) Studies in the physical properties of soils. II. A note on the cohesion developed by capillary forces in an ideal soil. *J. Agric. Sci*, **15,** 525–535.

Harnby, N. (1992) The mixing of cohesive powders. In: *Mixing in the Process Industries* (Eds N. Harnby, M.F. Edwards and A.W. Nienow), pp. 79–98. Butterworth-Heinemann Ltd, Oxford.

Hilhorst, M.A., Dirksen, C., Kampers, F.W.H. and **Feddes, R.A.** (2001) Dielectric relaxation of bound water versus soil matric pressure. *Soil Sci. Soc. Am J.*, **65,** 311–314.

McKenna Neuman, C. (2003) Effects of temperature and humidity upon the entrainment of sedimentary particles by wind. *Bound.-Lay. Meteorol.*, **108,** 61–89.

McKenna Neuman, C. and **Nickling, W.G.** (1989) A theoretical and wind tunnel investigation of the effect of capillary water on the entrainment of sediment by wind. *Can. J. Soil Sci.*, **69,** 79–96.

Nicholson, S. (2000) Land surface processes and Sahel climate. *Rev. Geophys.*, **38,** 117–139.

Orozco, A.A. (2000), *Fine particulate matter generation under controlled laboratory and wind tunnel conditions*. PhD Dissertation, Texas Tech University, Lubbock, TX.

Pope, C.A., Jr, Bates, D.V. and **Raizenne, M.E.** (1996) Health effects of particulate air pollution: time for reassessment?. *Env. Health Perspect.*, **103,** 472–480.

Ramanathan, V., Crutzen, P.J., Kiehl, J.T. and **Rosenfeld, D.** (2001) Aerosols, climate, and the hydrological cycle. *Science*, **294,** 2119–2124.

Ravi, S., D'Odorico, P., Over, T.M. and **Zobeck, T.M.** (2004) On the effect of air humidity on soil susceptibility to wind erosion: the case, 1999 of air-dry soils. *Geophys. Res. Lett.*, **31,** L09501, doi:10.1029/2004GL019485.

Saleh, A. and **Fryrear, D.W.** (1995) Threshold wind velocities of wet soils as affected by wind blown sand. *Soil Sci.*, **160,** 304–309.

Shao, Y. (2000) *Physics and Modelling of Wind Erosion*. Kluwer Academic Publishers, Dordrecht, 131 pp.

Shao, Y. and **H. Lu** (2000) A simple expression for wind erosion threshold friction velocity. *J. Geophys. Res.*, **105,** 22437–22443.

Stout, J.E. and **Zobeck, T.M.** (1997) Intermittent saltation. *Sedimentology*, **44,** 959–970.

USDA**. (2004)** *Natural Resources Conservation Service, Soil Survey Division, Official Soil Series Descriptions* [WWW document]. URL http://soils.usda.gov/technical/classification/osd/index.html [accessed on 14 December 2004].

Zobeck, T.M. and **Fryrear, D.W.** (1986) Chemical and physical characteristics of wind blown sediment. II. Chemical characteristics and total soil and nutrient discharge. *Trans. ASAE*, **29,** 1037–1041.

Zobeck, T.M., Fryrear, D.W. and **Pettit, R.D.** (1989) Management effects on wind-eroded sediment and plant nutrients. *J. Soil Water Cons.*, **44,** 160–163.

Manuscript received 13 May 2005; revision accepted 5 September 2005